Adult male rat hippocampus synthesizes estradiol from pregnenolone by cytochromes P45017α and P450 aromatase localized in neurons

Yasushi Hojo*[†], Taka-aki Hattori*[†], Taihei Enami*, Aizo Furukawa[†‡], Kumiko Suzuki*, Hiro-taka Ishii*, Hideo Mukai*[†], John H. Morrison[§], William G. M. Janssen[§], Shiro Kominami[¶], Nobuhiro Harada[∥], Tetsuya Kimoto*[†], and Suguru Kawato*[†]**

*Department of Biophysics and Life Sciences and [†]Core Research for Evolutional Science and Technology Project of Japan Science and Technology Corporation, Graduate School of Arts and Sciences, University of Tokyo at Komaba, Meguro, Tokyo 153, Japan; [‡]Department of Psychiatry, Tokyo Metropolitan Matsuzawa Hospital, 2-1-1 Kamikitazawa, Setagaya, Tokyo 156, Japan; [§]Kastor Neurobiology of Aging Laboratories, Fishberg Research Center for Neurobiology, Mount Sinai School of Medicine, New York, NY 10029; [¶]Faculty of Integrated Arts and Sciences, Hiroshima University, Higashi-hiroshima 739, Japan; and [∥]Department of Biochemistry, School of Medicine, Fujita Health University, Toyoake, Aichi 470, Japan

In adult mammalian brain, occurrence of the synthesis of estradiol from endogenous cholesterol has been doubted because of the inability to detect dehydroepiandrosterone synthase, P45017α. In adult male rat hippocampal formation, significant localization was demonstrated for both cytochromes P45017α and P450 aromatase, in pyramidal neurons in the CA1–CA3 regions, as well as in the granule cells in the dentate gyrus, by means of immunohistochemical staining of slices. Only a weak immunoreaction of these P450s was observed in astrocytes and oligodendrocytes. ImmunoGold electron microscopy revealed that P45017α and P450 aromatase were localized in pre- and postsynaptic compartments as well as in the endoplasmic reticulum in principal neurons. The expression of these cytochromes was further verified by using Western blot analysis and RT-PCR. Stimulation of hippocampal neurons with N-methyl-D-aspartate induced a significant net production of estradiol. Analysis of radioactive metabolites demonstrated the conversion from [^{3}H]pregnenolone to [^{3}H]estradiol through dehydroepiandrosterone and testosterone. This activity was abolished by the application of specific inhibitors of cytochrome P450s. Interestingly, estradiol was not significantly converted to other steroid metabolites. Taken together with our previous finding of a P450scc-containing neuronal system for pregnenolone synthesis, these results imply that 17β-estradiol is synthesized by P45017α and P450 aromatase localized in hippocampal neurons from endogenous cholesterol. This synthesis may be regulated by a glutamate-mediated synaptic communication that evokes Ca^{2+} signals.

The hippocampal formation, essentially involved in learning and memory processes, is known to be a target for the neuromodulatory actions of hormones produced in the gonads. As both estradiol and testosterone may reach the brain via blood circulation, and extensive studies have been performed to investigate their role in modulating hippocampal plasticity and function (1–4). Evidence is emerging that estrogen exerts not only the chronic/genomic effects but also a rapid/nongenomic influence on hippocampal synaptic plasticity (2, 5). In addition to endocrine-derived hormones, recent experiments have demonstrated that hippocampal neurons may also be exposed to locally synthesized brain neurosteroids, such as pregnenolone (PREG) and its sulfated ester (6–9). Dehydroepiandrosterone (DHEA) has been found in the mammalian brain at concentrations greater than that in plasma (6, 10). Because DHEA concentrations do not decrease after adrenalectomy and castration, many experiments have been performed with the aim of demonstrating the *de novo* synthesis of DHEA within the brain. DHEA biosynthesis has been demonstrated in cultured glial cells and neurons from the neonatal rat brain (11, 12). In the adult brain, however, a concrete demonstration of the synthesis of DHEA, androstenedione (AD), testosterone, or estradiol directly from endogenous cholesterol has yet to be reported. Sex steroids such as estradiol and testosterone, therefore, have not classically been considered to be "brain-derived neurosteroids." Furthermore, the localization and activity of cytochrome P45017α (CYP17) in adult mammalian brain has also not been demonstrated, despite many sophisticated studies employing immunohistochemistry, molecular biology, and enzyme activity assays (13–16). P45017α has, therefore, been regarded to be only transiently expressed in the brain at embryonic and neonatal stages (11, 12, 14). Recently, a few studies have reported the presence of cytochrome P450 aromatase (P450arom, CYP19) in the adult rat and human hippocampal formation (17, 18).

The present study was designed to examine, in the adult male hippocampus, the cellular localization of P45017α and P450arom and the endogenous metabolism of neurosteroids from PREG. Analyses revealed the neuronal localization of these P450s and the synthesis of DHEA, testosterone, and 17β-estradiol, which suggests their intracrine/paracrine actions on the plasticity of neurons in adult rat brain.

Materials and Methods

Animals. Adult male Wistar rats (3 months old, 210–250 g) were purchased from SLC Japan and Harlan Sprague–Dawley. All experiments using animals in this study were conducted according to the institutional guidelines.

Immunohistochemical Staining of Hippocampal Slices. Immunohistochemical staining was performed essentially as described in refs. 7 and 8. The hippocampi were frozen-sliced with a cryostat. After application of either anti-P45017α IgG (19), at 1/1,000 dilution or anti-P450arom IgG (20) at 1/1,000, the slices were incubated for 18–36 h. Biotinylated anti-rabbit IgG and streptavidin–horseradish peroxidase complex (Vector Laboratories) was applied. Immunoreactive cells were detected in diaminobenzidine-nickel. Fluorescence immunohistochemistry was performed by using streptavidin–Oregon Green 488. For detailed description of the procedures, see *Supporting Text*, which is published as supporting information on the PNAS web site.

Postembedding ImmunoGold Method for Electron Microscopy. Hippocampal slices were prepared by using a vibratome. Freeze substitution and low-temperature embedding of the specimens was performed as described (21). Slices were plunged into liquid propane and immersed in uranyl acetate solution. After polymerization of Lowicryl HM20 resin, ultrathin sections (80 nm

PHARMACOLOGY

thickness) were cut by using an ultramicrotome. For immuno-labeling, sections were incubated with primary antibody against P45017α (1:1,000) or P450arom (1:500) overnight and incubated with secondary gold-tagged (10 nm) Fab fragment in Tris-buffered saline. Sections were counterstained with 1% uranyl acetate and viewed on an electron microscope. For detailed description of the procedures, see *Supporting Text*.

Western Immunoblot Analysis. Microsomes were prepared as described in *Supporting Text* (8). After gel electrophoresis and the transfer to poly(vinylidene fluoride) membranes (Immobilon-P; Millipore), the blots were probed with antibodies against P45017α and P450arom at 1/5,000 dilution and incubated with biotinylated goat anti-rabbit IgG. The membranes were incubated with strepta-vidin–horseradish peroxidase complex. The protein bands were detected with ECL plus Western blotting detection reagents (Amersham Pharmacia).

RT-PCR and Southern Hybridization. The purified RNAs from rat tissues were reverse-transcribed by using a T-primed first-strand kit (Amersham Pharmacia) (22). Specific primer pairs and the PCR protocols are described in *Supporting Text*. For semiquantitative analysis (see ref. 23), the RT-PCR products were separated on 1.5% agarose gels, stained with ethidium bromide, and analyzed with a fluorescence gel scanner (Atto) and NIH IMAGE software, in comparison with standard curves obtained from PCR of diluted reverse transcribed products (between 1/100 and 1/10,000 in dilution), from testis, ovary, or liver. The PCR products were cloned into TA-cloning vector (Promega) and sequenced. The resulting sequence was identical to the reported cDNA sequences. These cloned products were used as DNA probes for Southern hybridization. After transfer of the RT-PCR products to nylon membrane, Southern hybridization was performed with ^{32}P-labeled cDNA probes for P45017α, P450arom, and GAPDH. Signals were measured by using a BAS-1000 Image analyzer (Fuji film).

HPLC Analysis. Procedures were essentially the same as described in ref. 8. Briefly, the hippocampal cubic slices were incubated with 5 × 10^6 cpm of [^{3}H]steroids at 28°C in a 1.2 mM Mg^{2+} physiological saline (pH 7.2, consisting of 5 mM Hepes, etc.), into which 95% O$_2$ gas was bubbled. [^{3}H]steroids (DHEA, estradiol, etc.) were purchased from New England Nuclear, and their specific activities were 22.5–105 Ci/mmol (1 Ci = 37 GBq). After termination of the reaction, the slices were homogenized. To extract steroid metabolites, ethyl acetate/hexane (3:2) was applied to the homogenates. The organic phase was collected by centrifugation, dried, dissolved in an elution solvent of HPLC, and filtrated. The metabolites were separated by using an HPLC system (Jasco, Tokyo). For detailed description of the procedures, see *Supporting Text*.

RIA Analysis. Procedures were essentially the same as described in ref. 8. Briefly, plasma was prepared from trunk blood collected from decapitated rats. The hippocampal cubic slices were incubated at 37°C in 0.1 mM Mg^{2+} physiological saline into which O$_2$ gas was bubbled. Extraction of steroids were performed as described in HPLC analysis. The estradiol or DHEA fractions were separated by using HPLC with solvent A, and reconstituted in a 0.1 M sodium phosphate buffer containing 0.1% gelatin. The concentration of steroids was measured by means of RIA, which was a competitive reaction assay, for example, between purified estradiol and exogenously added [^{3}H]estradiol against estradiol IgG. Anti-steroid IgG was from ICN. For a detailed description of the procedures, see *Supporting Text*.

Results

Localization and Presence of Cytochrome P450s. Light microscopic investigations of the immunohistochemical staining were performed to determine the cell-specific localization of P45017α and P450arom in the hippocampal formation of adult male rats. Intense
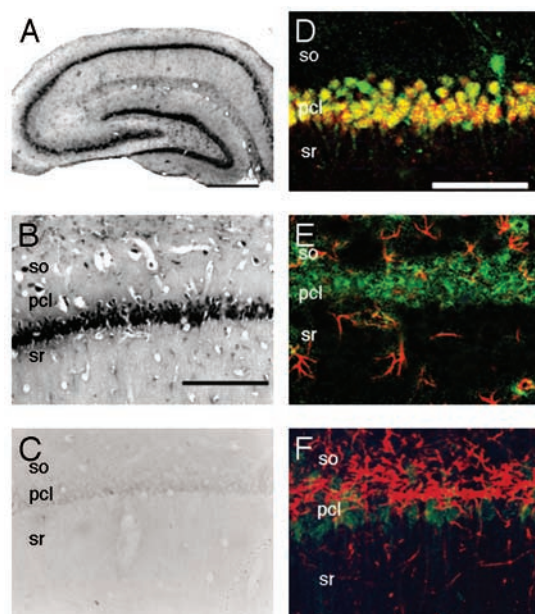

Fig. 1. Immunohistochemical staining of P45017α in the hippocampal formation of an adult male rat. (*A*) The coronal section of the whole hippocampal formation. (*B*) The CA1 region. (*C*) The CA1 stained with anti-P45017α IgG preadsorbed with purified P45017α. (*D*) Fluorescence dual staining of P45017α (green) and neuronal nuclear antigen (red). (*E*) Fluorescence dual staining of P45017α (green) and glial fibrillary acidic protein (red). (*F*) Fluorescence dual staining of P45017α (green) and myelin basic protein (red). In *D–F*, superimposed regions of green and red fluorescence are represented by yellow. so, stratum oriens; pcl, pyramidal cell layer; sr, stratum radiatum. (Scale bar, 800 μm for *A* and 120 μm for *B–F*.)

immunoreactions with anti-P45017α IgG (Fig. 1) and anti-P450arom IgG (Fig. 2) were restricted to pyramidal neurons in the CA1–CA3 regions and to granule cells in the dentate gyrus. The staining shows P45017α and P450arom to be distributed over the entire cell body, in general, and also along the dendrites of the pyramidal neurons in the CA3 region. Neurons were stained with IgG against neuronal nuclear antigen (NeuN). The colocalization of neurons with P45017α and P450arom was demonstrated by using fluorescence dual labeling procedures. Although the NeuN and P450 stainings were nearly superimposed, this was due to the
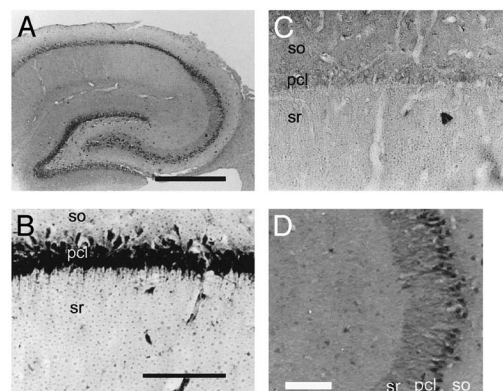

Fig. 2. Immunohistochemical staining of P450arom in the hippocampal formation of an adult male rat. (*A*) The coronal section of the whole hippocampal formation. (*B*) The CA1 region. (*C*) The CA1 stained with P450arom IgG preadsorbed with purified P450arom. (*D*) The CA3, where not only cell bodies but also processes of neurons are densely stained. so, stratum oriens; pcl, pyramidal cell layer; sr, stratum radiatum. (Scale bar, 800 μm for *A* and 120 μm for *B–D*.)

Fig. 4. Western immunoblot analysis of P45017α (*A*) and P450arom (*B*) in microsomes from adult rat. (*A*) Lung (50 μg protein), testis (1 μg), and hippocampus (50 μg). (*B*) Lung (50 μg protein), ovary (1 μg), and hippocampus (50 μg). Lung was used as a negative control.
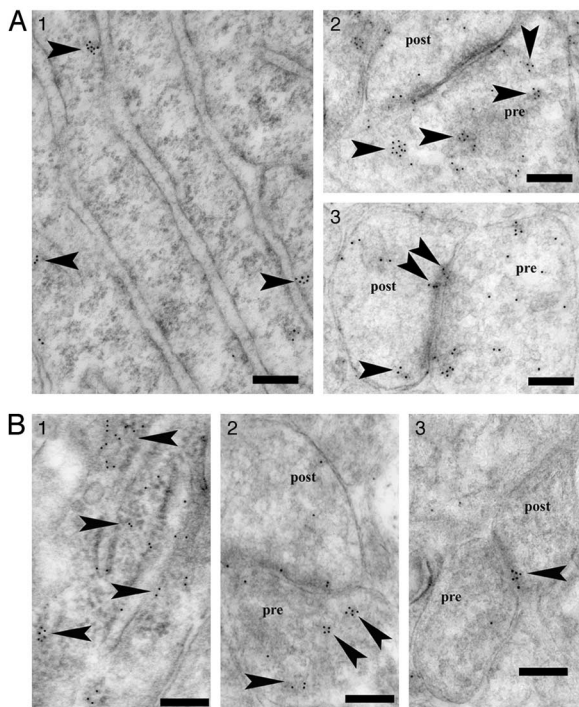
Fig. 3. Immunoelectron microscopic analysis of the distribution of P45017α (*A1–A3*) and P450arom (*B1–B3*) within axospinous synapses, in the strata radiatum of the hippocampal CA1 region at the central region of the rostrocaudal level. Gold particles (indicated with arrowheads) were observed to be localized in the endoplasmic reticulum (*A1* and *B1*), the presynaptic region (*A2* and *B2*), and the postsynaptic region (*A3* and *B3*) of pyramidal neurons. In the axon terminal (*A2* and *B2*), gold particles were associated with small synaptic vesicles (*A2* and *B2*). In dendritic spines, gold particles were found within the head of the spine (*A3* and *B3*). Pre, presynaptic region; Post, postsynaptic region. (Scale bar, 200 nm.)

localization of these cytochromes in the endoplasmic reticulum, distributed over the entire cell bodies, and thus did not indicate a nuclear localization of the cytochromes. Preadsorption of the antibody with an excess of purified guinea pig P45017α or human P450arom antigen (30 μg/ml) resulted in a complete disappearance of the immunoreactivity of these P450s, in all of the positively stained cells in the hippocampus.

The distribution of glial cells was investigated by the immuno-staining of marker proteins. Antibodies against glial fibrillary acidic protein (GFAP) of astrocytes, stained star-shaped cells in the strata radiatum, and oriens in the hippocampus. IgG against myelin basic protein (MBP) of oligodendrocytes stained many long fibril cells in the hippocampus. Most of the cells stained with GFAP and MBP IgG were lacking in immunoreactivity to IgG against P45017α and P450arom. This indicates that most of the P45017α- and P450arom-containing cells are neither astrocytes nor oligodendrocytes.

The neuronal localization of P450 was further clarified by ultra-structural investigations. An immunoelectron microscopic analysis using postembedding immunogold was performed to determine the subcellular localization of P45017α and P450arom in hippocampal neurons of adult male rats. P45017α (Fig. 3*A*) and P450arom (Fig. 3*B*) were localized not only in the endoplasmic reticulum but also in both the axon terminals and dendritic spines of principal neurons. Gold particles were clustered in the endoplasmic reticulum of neurons. Gold particles were also localized within the presynaptic compartments, as well as within the postsynaptic compartments. In the presynaptic terminals, gold particles were primarily associated with synaptic vesicles. In dendrites, gold particles were distributed within the cytoplasm of the head of the spine. In some cases, gold particles were affiliated within the postsynaptic density. Preadsorp-
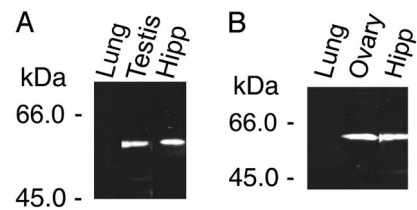
tion of the antibody with an excess of P45017α or P450arom antigen (30 μg/ml) resulted in a complete disappearance of the immuno-reactivity of these P450s, in all of the positively stained cells.

There were essentially no significant differences between P45017α and P450arom concerning their topographical distribution in neurons. Investigations were performed mainly in the stratum radiatum of the CA1; however, the intraneuronal distribution of gold particles was essentially identical in the CA1, CA3, and dentate gyrus.

The presence of P45017α and P450arom proteins was verified by Western immunoblot analysis. In hippocampal microsomes, single protein bands were observed for P45017α and P450arom (Fig. 4). The concentration of P45017α and P450arom was ≈1/100th to 1/200th of that typical of the testis (P45017α) and ovary (P450arom). The electrophoretic mobility of the P45017α and P450arom bands indicated a molecular mass of ≈57 kDa and 58 kDa, respectively. These molecular masses were approximately equal to those in testis and ovary. Protein bands disappeared when either antibodies were preadsorbed with purified P450 antigens (30 μg/ml).

The level of mRNA transcripts for P45017α and P450arom was investigated by using RT-PCR analyses. The relative number of P450 transcripts expressed in the hippocampus (Fig. 5, lane 5) from adult male rats was demonstrated to be ≈1/200th to 1/300th of those expressed in the testis and ovary, for P45017α and P450arom, respectively. The mRNA levels for P45017α and P450arom in the hypothalamus (Fig. 5, lane 6) were slightly greater (by ≈1.5-fold) than those obtained in the hippocampus. On the other hand, the level of P45017α mRNA in the cerebral cortex (Fig. 5, lane 4) and cerebellum (Fig. 5, lane 7), was $<10^{-4}$ and 10^{-3}, respectively relative to levels observed in the testis. The level of P450arom mRNA, relative to levels in the ovary, was ≈1/500 in the cerebral cortex (Fig. 5, lane 4) and cerebellum (Fig. 5, lane 7).

The expression level of mRNA transcripts for 17β-hydroxy-

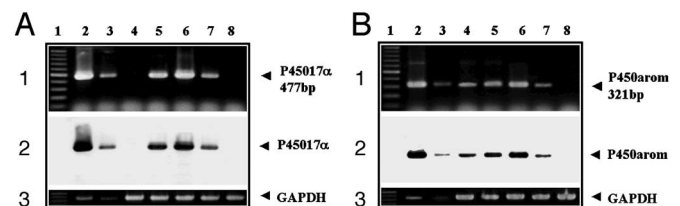**Fig. 5.** RT-PCR analysis of mRNAs for P45017α (*A*) and P450arom (*B*) in the adult rat. The RT-PCR products (50 ng each) were visualized with ethidium bromide in *Top*. (*A*) Lane 1, marker (100-bp ladder); lane 2, testis diluted at 1/100; lane 3, testis diluted at 1/1,000; lane 4, cerebral cortex; lane 5, hippocampus; lane 6, hypothalamus; lane 7, cerebellum; lane 8, peripheral blood leukocytes. (*B*) Lane 1, marker; lane 2, ovary diluted at 1/100; lane 3, ovary diluted at 1/1,000; lane 4, cerebral cortex; lane 5, hippocampus; lane 6, hypothalamus; lane 7, cerebellum; lane 8, liver. Peripheral blood leukocytes and liver were used as the negative controls. (*Middle*) Southern hybridizations. (*Bottom*) Ethidium bromide staining of GAPDH.
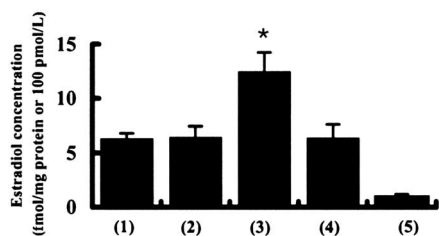
Fig. 6. RIA analysis of estradiol concentrations in adult male rats. Estradiol concentration in the hippocampus before incubation (basal) (column 1), the hippocampus after a 30-min incubation without NMDA (column 2), the hippocampus after a 30-min incubation with 100 μM NMDA (column 3), the hippocampus after a 30-min incubation with 100 μM NMDA in the presence of MK-801 (column 4), and plasma (column 5). The vertical axis indicates the estradiol concentration in fmol/mg protein for the hippocampus (columns 1–4) and in fmol/μl for plasma (column 5). The significance of the NMDA-induced production of estradiol was confirmed by using the Student t test (*, $P < 0.05$). The data represent an average over three independent experiments.

steroid dehydrogenase (17β-HSD) (types 1–4) was also investigated by using RT-PCR (data not shown). The level of 17β-HSD mRNA observed in the hippocampus was $\approx$1/10th relative to the level in the ovary for 17β-HSD (type 1), 1/200th to 1/300th relative to the level in the testis for 17β-HSD (type 3), roughly the same relative to the level in the liver for 17β-HSD (type 4), and $<10^{-3}$ for 17β-HSD (type 2) relative to the level in the liver.

Steroid Metabolism Assay. The synthesis of estradiol in hippocampal slices was examined by means of a specific RIA using estradiol antibody (ICN) (Fig. 6). The basal concentration of estradiol observed in the hippocampus was 0.60 $\pm$ 0.05 fmol/mg wet weight (6.3 $\pm$ 0.5 fmol/mg protein; mean $\pm$ SEM from three independent experiments). The estradiol basal concentration in the plasma was 0.098 $\pm$ 0.039 fmol/μl ($\approx$1.02 fmol/mg protein or 0.098 fmol/mg

wet weight), a value considerably lower than that observed in the hippocampus. The N-methyl-D-aspartate (NMDA)-inducible production of estradiol was measured by stimulating hippocampal slices with 100 μM NMDA (Biomol) for 30 min, at 37°C in a 0.1 mM Mg^{2+} medium. This treatment increased the concentration of estradiol to 1.35 $\pm$ 0.18 fmol/mg wet weight (13.0 $\pm$ 1.7 fmol/mg protein), which is nearly twice the estradiol level in hippocampal slices incubated for 30 min without NMDA. Stimulation of net estradiol production with NMDA was completely suppressed by the application of 50 μM MK-801 (a specific blocker of NMDA receptors, Sigma). This enhancement in estradiol synthesis may be due to an increase in the NMDA receptor-mediated Ca^{2+} influx that drives the transport of cholesterol to the inner membrane of mitochondria, followed by a cascade of steroidogenesis (7). The basal concentration of DHEA was also measured in the hippocampus and plasma. The concentration of DHEA was 0.28 $\pm$ 0.07 fmol/mg wet weight (2.7 $\pm$ 0.7 fmol/mg protein) in the hippocampus, and 0.075 $\pm$ 0.036 fmol/μl in plasma. These values are in reasonable agreement with previous publications using DHEA extracts from the whole brain (6).

To analyze the pathway of steroidogenesis, the metabolism of radioactive steroids in hippocampal slices was investigated by using HPLC. To observe the conversion of PREG to DHEA, hippocampal cubic slices from adult male rats were incubated for 0, 1, 3, and 5 h at 28°C, using 5 × 10^6 cpm of [7-^{3}H]PREG as a precursor. Careful attention was given to the removal of all fats from the hippocampal slices during the purification of steroids, before the application to HPLC. A portion of the purified radioactive metabolites (total of 10^6 cpm) was analyzed with an HPLC system, which used an elution liquid composed of hexane/isopropanol/acetic acid (97:3:1) (solvent A). The principal radioactive peak in the tritiated metabolite exhibited a retention time of $\approx$9.5 min, which was the same as that of [^{14}C]DHEA used as a standard (Fig. 7A). A time-dependent increase in the [^{3}H]DHEA fractions was observed over a period of 5 h (Fig. 8A, which is published as supporting
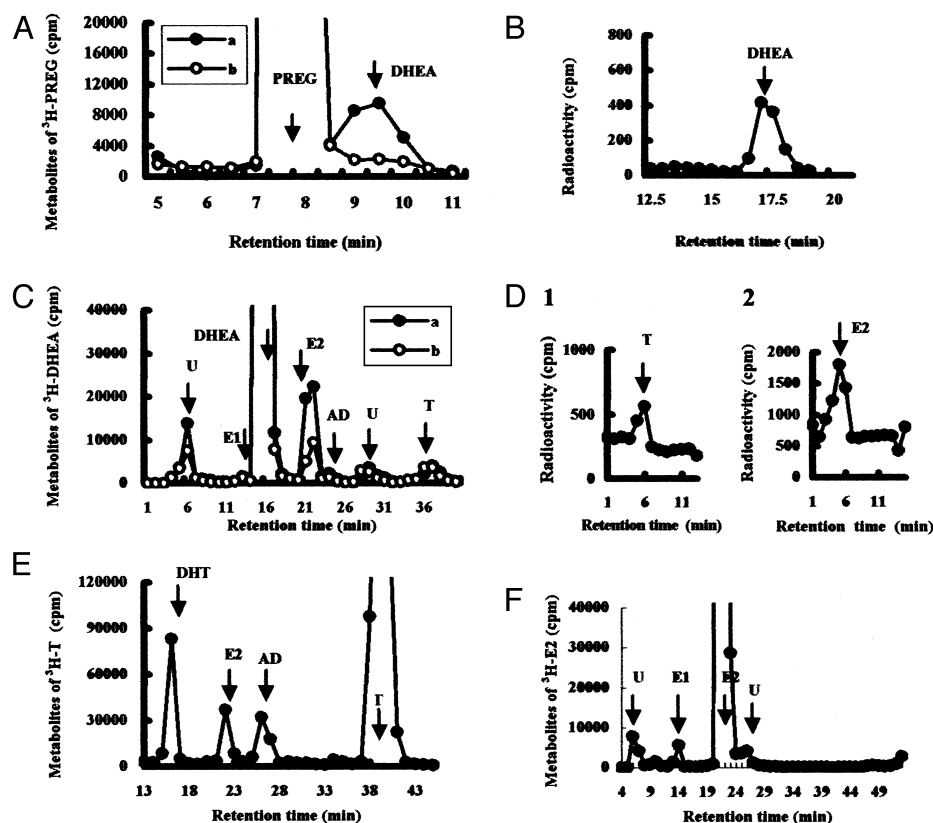

Fig. 7. HPLC analysis of steroid metabolism in adult rat hippocampal slices. A total of 10^6 cpm purified metabolites were applied to HPLC. (A) HPLC profiles of [^{3}H]PREG metabolites using elution solvent A. Slices were incubated for 5 h in the absence (line a) or in the presence (line b) of SU-10603. (B) Reverse-phase HPLC (solvent C) of [^{3}H]DHEA fractions from line a in A. (C) Profiles of [^{3}H]DHEA metabolites (solvent B) in the absence (line a) or in the presence (line b) of fadrozole, after incubation of slices for 5 h. (D) Reverse-phase HPLC (solvent C) of [^{3}H]testosterone ($D1$) and [^{3}H]estradiol ($D2$) taken from peaks T and E2, respectively, in C. (E) Profiles (solvent B) of [^{3}H]testosterone metabolites after incubation of slices for 5 h. (F) Profiles (solvent B) of [^{3}H]estradiol metabolites after a 5-h incubation. The arrows designate the elution peak position of the standard [^{14}C]steroid with abbreviations: E1 (estrone), T (testosterone), and E2 (estradiol). ''U'' designates unknown metabolites. The vertical axis indicates ^{3}H radioactivity (cpm). The retention time of the (same) standard [^{14}C]steroid differed slightly among C, E, and F due to the different silica gel columns used. More than three independent experiments were performed for each of these analyses.

information on the PNAS web site). Analysis of the steroid extract (adjusted to a total of 10^6 cpm) indicated that the amount of [^{3}H]DHEA (product), relative to [^{3}H]PREG (substrate), increased from $0.0 \times 10^4/1.0 \times 10^6$ (0 h) to $1.0 \times 10^4/0.98 \times 10^6$ (1 h), $2.9 \times 10^4/0.97 \times 10^6$ (3 h), and $4.6 \times 10^4/0.96 \times 10^6$ (5 h). Note that trilostane (Mochida) was included in these experiments to facilitate observation of the net production of [^{3}H]DHEA by inhibiting 3β-hydroxysteroid dehydrogenase (3β-HSD). Trilostane prevents the conversion of DHEA to AD and of PREG to progesterone. The application of a specific inhibitor of P45017α, SU-10603 (Novartis) at 10 μM, reduced the production of [^{3}H]DHEA to $\approx$21% of the control value. To exclude the possibility of contamination from other radioactive metabolites, the three fractions having a retention time of 9–10 min were combined and subjected to a second round of HPLC analysis. The column was eluted with a different elution solvent B (hexane/isopropanol/acetic acid = 98:2:1) for the normal phase HPLC (Fig. 8*B*), and with solvent C (acetonitrile/H$_2$O = 40:60) for the reverse-phase HPLC (Fig. 7*B*), to improve the resolution. A single radioactive peak of [^{3}H]metabolite having the same retention time as that of [^{14}C]DHEA was observed in this second round of HPLC. These results indicate the significant enzymatic activity of P45017α in the hippocampus, which is responsible for the conversion of PREG to DHEA.

To investigate the conversion of DHEA to testosterone and estradiol, hippocampal slices were incubated with 5×10^6 cpm of [1,2,6,7-^{3}H]DHEA for 5 h at 28°C, and the purified metabolites (total of 10^6 cpm) were analyzed by using HPLC. When elution solvent B was used, several eluent peaks were observed (Fig. 7*C*). The eluent peak with a retention time of 37 min was designated as testosterone by comparison with the standard [^{14}C]testosterone. The eluent peak exhibiting a retention time of 21–22 min was close to the position of [^{14}C]estradiol. To improve the resolution, these fractions were collected and subjected to a second round of HPLC analysis using solvent D (hexane/isopropanol/acetic acid = 99:1:1). A single peak, with a retention time of 51 min, was observed, which is in good agreement with [^{14}C]estradiol (Fig. 8*C*). An additional round of analysis, using reverse-phase HPLC and solvent C, was performed for the HPLC fractions corresponding to estradiol, testosterone, and AD. These metabolites were again observed to elute at the same positions obtained for the standard [^{14}C]steroids (Fig. 7*D*). Analysis of the steroid extract (10^6 cpm) indicated that the relative amount of [^{3}H]estradiol (product) to [^{3}H]DHEA (substrate) increased from $0.0 \times 10^4/1.0 \times 10^6$ (0 h) to $3.5 \times 10^4/0.90 \times 10^6$ (1 h), $5.5 \times 10^4/0.88 \times 10^6$ (3 h) and $6.4 \times 10^4/0.86 \times 10^6$ (5 h).

To confirm the participation of P450arom in estradiol synthesis, fadrozole (Novartis) was used to inhibit the activity of P450arom. A 30-min preincubation with 100 μM fadrozole, applied before the addition of [^{3}H]DHEA, suppressed the conversion of [^{3}H]DHEA to estradiol considerably (to $\approx$34% of the control), but had no suppressive effect on its conversion to testosterone (to $\approx$102% of the control) (Fig. 7*C*). The conversion from testosterone to estradiol and dihydrotestosterone (DHT) was then investigated. Hippocampal slices were incubated with [1,2,6,7-^{3}H]testosterone (5×10^6 cpm) for 0, 1, 2, 3, 4, and 5 h at 28°C, and the purified metabolites (total of 10^6 cpm) were analyzed with HPLC using solvent B (Fig. 7*E*). A time-dependent increase in [^{3}H]estradiol, [^{3}H]DHT, and [^{3}H]AD was observed (Fig. 8*D*). Analysis of the steroid extracts (10^6 cpm) indicted that the relative amount of [^{3}H]estradiol (product) to [^{3}H]testosterone (substrate) increased from $0.0 \times 10^4/1.0 \times 10^6$ (0 h) to $0.7 \times 10^4/0.90 \times 10^6$ (1 h), $1.9 \times 10^4/0.87 \times 10^6$ (3 h) and $3.8 \times 10^4/0.84 \times 10^6$ (5 h). The absence of other contaminating metabolites in these estradiol fractions was confirmed by means of a second round of HPLC using solvent C (for normal phase HPLC) and D (for reverse-phase HPLC).

HPLC analysis of AD and estrone metabolites are described in *Supporting Text*. Finally, the conversion of estradiol to other metabolites was also investigated by incubating [2,4,6,7-

[^{3}H]estradiol (5×10^6 cpm) with hippocampal slices for 5 h. Only very small amounts of metabolites such as estrone and testosterone were observed (Fig. 7*F*), suggesting that estradiol was not significantly inactivated but may remain stable.

Discussion

Our results not only demonstrated the distribution of P45017α and P450arom in pyramidal and granule neurons at the light microscopic level (Figs. 1 and 2), but also indicated that these P450 proteins were specifically localized in pre- and post-synaptic locations and the endoplasmic reticulum of these neurons by electron microscopy, with a single molecule (gold particle) resolution (Fig. 3). These findings, combined with the results of steroid metabolism assays, strongly suggest that estradiol is endogenously synthesized in neurons from cholesterol in the hippocampal formation. These results indicate the need to reconsider the belief that these sex steroids are produced only in the gonads and reach the target brain via blood circulation. Rather, such steroids may be produced endogenously in the adult brain, where they play an essential role in the plasticity and protection of neurons.

Pathway of Steroidogenesis in the Hippocampus. In our previous work, the steroid synthesis was triggered by exposing neurons to NMDA, which induced a Ca^{2+} influx through the NMDA receptors and resulted in the significant production of PREG(s) (5, 7). A pool of full-length (37-kDa) steroidogenic acute regulatory protein (StAR) was processed to the truncated 30-kDa StAR upon NMDA stimulation (7). The expression of essential steroidogenic proteins [StAR, P450scc (CYP11A1), and 3β-HSD] in the hippocampal principal neurons was demonstrated by means of immunostaining and Western blot analysis (7–9) or by *in situ* hybridization (17, 22). The presence of mRNAs for 17β-HSD types 1–4 has been demonstrated in the human hippocampus (24). In the rat hippocampus, 17β-HSD (type 1) has been shown to be localized in neurons by immunostaining (25). Previous studies have shown the immunoreactivity of 5α-reductase in the rat hippocampus (16, 26).

In combination with these results, the current observations suggest that hippocampal neurons are equipped with a set of enzymes to catalyze the synthesis of estradiol from cholesterol. Neurosteroid synthesis may therefore proceed in the following manner. First, cholesterol is transported with StAR into the inner membrane of mitochondria, and converted to PREG by P450scc. After reaching the microsomes, P45017α converts PREG to DHEA. Then DHEA to AD by 3β-HSD, 17β-HSD (type 3) catalyzes the conversion of AD to testosterone. This is followed by a further transformation to estradiol by P450arom. It appears that estradiol is also formed by 17β-HSD (type 1) from estrone, which is converted from AD by P450arom.

The rate of production of steroid metabolites was rather low. The amount of [^{3}H]DHEA formed from [^{3}H]PREG, that of [^{3}H]estradiol from [^{3}H]DHEA, and that of [^{3}H]estradiol from [^{3}H]testosterone each represented $\approx$4.6–6.4% of the total radioactivity obtained by using [^{3}H]steroid precursors, observed after 5-h incubation (Fig. 7). Several reasons are considered for this. First, the binding of exogenously applied [^{3}H]steroid to P450s in hippocampal slices is likely to be very inefficient, as such steroids must penetrate deeply into cells in the thick slices to reach enzymes, without being absorbed by nonspecific binding to hydrophobic membranes, and replace endogenous steroid substrates already bound to the enzymes. Second, the conversion rate from [^{3}H]PREG to [^{3}H]DHEA by P45017α may indeed be extremely low; as a result, no previous study could detect this low activity. Third, not only [^{3}H]DHEA but also other steroids such as sulfated DHEA and 7-hydroxyDHEA (27) may be produced in parallel from [^{3}H]PREG. Fourth, [^{3}H]estradiol is not a unique metabolite from [^{3}H]testosterone, but DHT and other steroids may also be produced in parallel. These multiple pathways, including backward reactions, may be a primary reason of the observed low efficiency of steroid metabolism, because of the

presence of sulfotransferase, 5α-reductase, and cytochrome P4507b (16, 26, 28). These factors could reduce the rate of production for [³H]DHEA and [³H]estradiol to 4.6–6.4% of the total radioactivity.

To verify that the observed low levels of radioactive metabolites were real products, we performed a set of control experiments. We observed a considerable decrease in [³H]DHEA production by the presence of SU-10603, inhibitor of P45017α (Fig. 7A). In addition, estradiol production was suppressed considerably by the presence of fadrozole, an inhibitor of P450arom (Fig. 7C). These results indicate that the observed steroid metabolite levels are above the detection limit of the HPLC analysis. The background radioactivity in the HPLC profiles in Fig. 7 was <300 cpm at any position, using hippocampal slices fixed with paraformaldehyde to inactivate steroidogenic enzymes before incubation with ³H-substrate steroids.

Glial cells have been considered to play an important role in neurosteroidogenesis, as many reports have indicated the presence of mRNA and steroidogenic activity for P450scc, P45017α, 3β-HSD, and 17β-HSD in cultures of astrocytes and oligodendrocytes (6, 11, 12, 29, 30). Based on these studies, the following steroidogenic sequence is suggested in the neonatal rat brain. The primary source of PREG is the oligodendrocytes. PREG is then transferred to the astrocytes, where it is converted to DHEA, and further metabolized to sex steroids (11, 12). It should be noted, however, that these studies, which use primary glial cell cultures, can be performed only for embryonic and neonatal brain. As a result, direct information is not available from these studies regarding the biosynthesis of neurosteroids in adult rat brain. The possibility of glial steroidogenesis in the adult hippocampal formation cannot be excluded by the present study, as a weak staining of P450scc (7), P45017α, and P450arom was observed in some glia-like cells.

Previous Understanding of P45017α and P450arom in the Brain. A direct demonstration of the neuronal synthesis of DHEA in adult mammalian brain has not previously been reported, although the presence of significant amounts of DHEA had been noted (15, 10). It has therefore been assumed that DHEA and the sex steroids are supplied to the brain via the blood circulation (6, 15, 20). As reported in a number of studies, the absence of P45017α and its activity in the brain of adult mammals has discouraged the investigation of the endogenous synthesis of sex steroids and DHEA in adult brain (13–16). Incubations of [³H]PREG with brain slices and microsomes from rat and mouse, had failed to produce [³H]DHEA (15). Moreover, many attempts to demonstrate the immunohistochemical reactivity for P45017α in the rat brain had been unsuccessful (13). mRNAs for P45017α had not been detected in adult rat brain by either RNase protection assays or RT-PCR (14). The expression of the mRNA for P45017α had been reported by many laboratories as only transient, occurring during rat embryonic and neonatal development (11, 12, 31). Although a similar level of

P45017α mRNA had been reported in both astrocytes and neurons in primary cultures from the brain of neonatal rats, neurons had exhibited a much lower metabolic activity than astrocytes for the conversion of PREG to DHEA (11, 12). Such investigations, which use primary cell cultures, are not possible for adult brains, because cells from adult brains cannot be cell cultured.

Our observation of a significant amount of P45017α mRNA was achieved due to (i) a careful design of primers to not include sequences that may form stable loops, inhibiting binding to mRNA, (ii) the use of isolated rat hippocampal formation, rather than brain mixtures where the cortex did not express P45017α mRNA, and (iii) the considerable improvement in the last few years of the commercially available enzymes such as Taq polymerase used for RT-PCR.

The role of P450arom in the hippocampus had also not been well elucidated, primarily because many studies had indicated the absence of P450arom in the adult rat and mouse hippocampus (20, 32). Recently, however, the significant expression of mRNA for P450arom in the pyramidal and granule neurons of the adult rat hippocampus has been demonstrated by using in situ hybridization (17). The level of the mRNA expression in the adult mouse hippocampus was approximately half of that in neonatal stages (23). The activity of P450arom has been suggested in the adult male rat hippocampus based on the results of the testosterone-induced protection of the hippocampal neuronal death induced by the domoic acid-treatments (3).

Modulation by Estradiol of Hippocampal Neurons. Investigations have been focused on female rats regarding the chronic, delayed effects of estradiol on synaptic plasticity. For example, the dendritic spine density in pyramidal neurons is sensitive to the estrous cycle (1, 33) and also to experimentally induced estrogen depletion and replacement, which serve to modulate estrogen levels in blood circulation (4). Estradiol also induces rapid effects. A 20-min preperfusion of 1–10 nM estradiol induced the rapid modulation of long-term potentiation of the CA1 neurons in the hippocampal slices (2). Our elucidation of the estradiol-synthesis in principal neurons, which begins with cholesterol, introduces an essentially a new supply of brain neurosteroids, in addition to gonads. Estradiol synthesis may be dependent on NMDA receptor-mediated Ca²⁺ influx, thereby dependent on synaptic communication (5, 7). The concentration of endogenously synthesized estradiol by NMDA stimulation (≈0.75 nM; see Fig. 6, column 3) should be sufficient to modulate these neuronal activities, because the local concentration of estradiol (at the site of synthesis) may transiently be an order of magnitude higher than the mean concentration of 0.75 nM.

1. Woolley, C. S., Weiland, N. G., McEwen, B. S. & Schwartzkroin, P. A. (1997) J. Neurosci. **17,** 1848–1859.
2. Foy, M. R. Xu, J. Xie, X. Brinton, R. D. Thompson, R. F. & Berger, T. W. (1999) J. Neurophisiol. **81,** 925–929.
3. Azcoitia, I., Sierra, A., Veiga, S., Honda, S., Harada, N. & Garcia-Segura, L. M. (2001) J. Neurobiol. **47,** 318–329.
4. Pozzo-Miller, L. D., Inoue, T. & Murphy, D. D. (1999) J. Neurophysiol. **81,** 1404–1411.
5. Shibuya, K., Takata, N., Hojo, Y., Furukawa, A., Yasumatsu, N., Kimoto, T., Enami, T., Suzuki, K., Tanabe, N., Ishii, H., et al. (2002) Biochim. Biophys. Acta **25462,** 1–16.
6. Baulieu, E. E. (1997) Recent Prog. Horm. Res. **52,** 1–32.
7. Kimoto, T., Tsurugizawa, T., Ohta, Y., Makino, J., Tamura, H., Hojo, Y., Takata, N. & Kawato, S. (2001) Endocrinology **142,** 3578–3589.
8. Kawato, S., Hojo, Y. & Kimoto, T. (2002) Methods Enzymol. **357,** 241–249.
9. Kawato, S., Yamada, M. & Kimoto, T. (2003) Adv. Biophys. **37,** 1–48.
10. Corpechot, C., Robel, P., Axelson, M., Sjovall, J. & Baulieu, E. E. (1981) Proc. Natl. Acad. Sci. USA **78,** 4704–4707.
11. Zwain, I. H. & Yen, S. S. C. (1999) Endocrinology **140,** 880–887.
12. Zwain, I. H. & Yen, S. S. C. (1999) Endocrinology **140,** 3843–3852.
13. Le Goascogne, C., Sananes, N., Gouezou, M., Takemori, S., Kominami, S., Baulieu, E. E. & Robel, P. (1991) J. Reprod. Fertil. **93,** 609–622.
14. Mellon, S. H. & Deschepper, C. F. (1993) Brain Res. **629,** 283–292.
15. Baulieu, E. E. & Robel, P. (1998) Proc. Natl. Acad. Sci. USA **95,** 4089–4091.
16. Mensah-Nyagan, A. G., Do-Rego, J. L., Beaujean, D., Luu-The, V., Pelletier, G. & Vaudry, H. (1999) Pharm. Rev. **51,** 63–81.
17. Wehrenberg, U., Prange-Kiel, J. & Rune, G. M. (2001) J. Neurochem. **76,** 1879–1886.
18. Stoffel-Wagner, B., Watzka, M., Schramm, J., Bidlingmaier, F. & Klingmuller, D. (1999) J. Steroid Biochem. Mol. Biol. **70,** 237–241.
19. Shinzawa, K., Ishibashi, S., Murakoshi, M., Watanabe, K., Kominami, S., Kawahara, A. & Takemori, S. (1988) J. Endocrinol. **119,** 191–200.
20. Jakab, R. L., Horvath, T. L., Leranth, C., Harada, N. & Naftolin, F. (1993) J. Steroid Biochem. Mol. Biol. **44,** 481–498.
21. Adams, M. M., Shah, R. A., Janssen, W. G. M. & Morrison, J. H. (2001) Proc. Nat. Acad. Sci. USA, **98,** 8071–8076.
22. Furukawa, A., Miyatake, A., Ohnishi, T. & Ichikawa, Y. (1998) J. Neurochem. **71,** 2231–2238.
23. Ivanova, T. & Beyer, C., (2000) Cell Tissue Res. **300,** 231–237.
24. Beyenburg, S., Watzka, M., Blumcke, I., Schramm, J., Bidlingmaier, F., Elger, C. E. & Stoffel-Wagner, B. (2000) Epilepsy Res. **41,** 83–91.
25. Pelletier, G., Luu-The, V. & Labrie, F. (1995) Brain Res. **704,** 233–239.
26. Melcangi, R. C., Cellotti, P., Castano, P. & Martini, L. (1993) Endocrinology **132,** 1252–1259.
27. Jellinck, P., Lee, S. J. & McEwen, B S., (2001) Steroid Biochem. Mol. Biol. **78,** 313–317.
28. Rose, K., Stapleton, G., Dott, K., Kieny, M. P., Best, R., Schwarz, M., Russel, D. W., Bjorkhem, I., Seckl, J. & Lathe, R. (1997) Proc. Natl. Acad. Sci. USA **94,** 4925–4930.
29. Jung-Testas, I., Hu, Z. Y., Baulieu, E. E. & Robel, P. (1989) Endocrinology **125,** 2083–2091.
30. Papadopoulos, V. (1993) Endocr. Rev. **14,** 222–240.
31. Compagnone, N. A., Bulfone, A., Rubenstein, J. L. R. & Mellon, S. H. (1995) Endocrinology **136,** 5212–5223.
32. Lauber, M. E. & Lichtensteiger, W. (1994) Endocrinology **135,** 1611–1668.
33. Woolley, C. S. & McEwen, B. S. (1994) J. Neurosci. **14,** 7680–7687.

Supporting Text

Materials and Methods

Immunohistochemical Staining of Hippocampal Slices. Rat hippocampal slices were prepared from animals deeply anesthetized with pentobarbital and perfused transcardially with a PBS (0.1 M phosphate buffer and 0.14 M NaCl, pH 7.3), followed by fixative solution of 4% paraformaldehyde. The hippocampi were postfixed, cryoprotected, and frozen-sliced coronally with a cryostat (Leica).

Staining for P450 was performed by using the avidin-biotin-peroxidase complex technique. After application of either purified anti-guinea pig P45017α IgG (1) at 1:1,000 dilution or purified anti-human cytochrome P450 aromatase (P450arom) IgG (2) at 1:1,000 dilution, the slices were incubated for 18-36 h at 4° C, in the presence of 0.5% Triton X-100. Biotinylated anti-rabbit IgG (1:1,000) and streptavidin-horseradish peroxidase complex (Vector Laboratories) was applied. Immunoreactive products were detected in a solution of diaminobenzidine with ammonium nickel sulfate. After embedding in Entellan Neu (Merck), the immunoreactive cells were examined under microscope. Fluorescence immunohistochemistry was carried out using streptavidin-Oregon Green 488 (Molecular Probes) instead of the avidin-peroxidase complex. Neurons, astroglial cells, and oligodendroglial cells were visualized by using monoclonal antibodies for NeuN (1:100), glial fibrillary acidic protein (GFAP) (1:3,000) and myelin basic protein (MBP) (1:10) (Chemicon), respectively, followed by the application of Cy3-labeled anti-mouse IgG (Jackson ImmunoResearch). Fluorescence signals were observed by using a MRC-1024 confocal microscope (Bio-Rad).

Postembedding ImmunoGold Method for Electron Microscopy. Rat hippocampal slices were prepared in essentially the same manner as that for the immunohistochemical staining, except for slicing at 4° C using a vibratome (Leica) instead of frozen slicing. Slices were cryoprotected in glycerol, and plunged into liquid propane cooled by liquid nitrogen in a Universal Cryofixation System KF80 (Reichert-Jung). The samples were immersed in uranyl acetate in anhydrous methanol (-90° C, 24 h) in a cryosubstitution AFS unit (Leica). After the temperature increase, the samples were washed and infiltrated with Lowicryl HM20 resin (Electron Microscopy Sciences) at -45° C with a progressive increase in the ratio of resin to methanol. Polymerization was performed with ultraviolet light. Ultrathin sections (80 nm in thickness) were cut by using a Reichert-Jung ultramicrotome and mounted on nickel mesh grids. The mesh grids with ultrathin sections were treated with NaOH in ethanol, and incubated in the solution containing 0.1% sodium borohydride and 50 mM glycine, and then in Tris-buffered saline (TBS). For immunolabeling, sections were incubated with primary antibody for P45017α (1:1,000) or P450arom (1:500) in the above diluent overnight, and incubated with secondary gold-tagged (10 nm) Fab fragment in TBS (2% serum albumin and polyethyleneglycol 20,000; 5 mg per 1 ml). Sections were washed, counterstained with 1% uranyl acetate and Reynolds lead citrate, and viewed on a JEOL 1200EX electron microscope. Images were captured by using the Advantage charge coupled device (CCD) camera (Advanced Microscopy Techniques, Danvers, MA). Controls omitting the primary antibody were performed, and no ImmunoGold labeling was observed. A search for ImmunoGold-labeled P450 was performed for at least 30 synapses per each rat.

Microsome Preparation for Western Immunoblot Analysis. The rat hippocampus, testis, ovary, and lung are excised, minced, and homogenized in a glass-Teflon homogenizer at 4° C in the homogenization buffer [50 mM potassium phosphate buffer (pH 7.4), 250 mM sucrose, 5 mM EDTA, 0.5 mM phenylmethylsulfonylfluoride, 0.1 mM leupeptin (Sigma) and 3 mM 2-mercaptoethanol]. After the removal of the nucleic fractions and mitochondria, the microsomal fractions were pelleted by centrifugation at $105,000 \times g$. Purification is repeated to obtain the final microsomal fractions. The microsomes were diluted to 10 mg of protein per ml with a Tris buffer composed of 62.5 mM Tris·HCl (pH 6.8), 6% sodium dodecylsulfate, 5% sucrose, 5% 2-mercaptoethanol and 0.01% bromophenol blue. The samples are denaturated for 5 min at 90° C and subjected to electrophoresis. Ten percent polyacrylamide gels are employed.

Specific Primer Pairs Used for RT-PCR and the PCR Protocols. P45017α, 5'-TGGGGCGGGCATAGAGACAACT-3' (forward) and 5'-AGCAAGGCCGTGAAGACAAAGAGC-3' (reverse); P450arom, 5'-TATGCACGTCACTCTACCCACTCAAG-3' (forward) and 5'-TCCAATCCCCATCCACAAGAATC-3' (reverse); 17β -hydroxysteroid dehydrogenase (17β -HSD) type 1, ACTCCGGGCGTGTGCTGGTGA (forward) and GGCGTGTCTGGATCCCCTGAAACTT (reverse); 17β -HSD type2, GCCGCCTACGCCTCCACGAA (forward) and CCGCGAAGCAGATCCACAGGTAAGTC (reverse); 17β -HSD type3, CTCCCCAACCTGCTCCCAAGTC (forward) and CAAGGCAGCCACAGGTTTCAGC (reverse); 17β-HSD type 4, TCGGAGTAGGAGCTTCAGTCAAAAAT (forward) and TGCAGAAAACCCAAAAGTACATAATCC (reverse).

The PCR protocols comprised application of a 30-sec denaturation period at 95° C, a 20 sec annealing period at 62☐☐ C (P45017α), 56° C (P450arom), 63° C (17β -HSD types 1 and 2), 59.5° C (17β -HSD type 3), and 56☐☐ C (17β -HSD type 4), and a 30-sec extension at 72˙C, for 37 cycles (P45017α), 35 cycles (P450arom), 38 cycles (17β -HSD types 1 and 3), 40 cycles (17β -HSD type 2) and 30 cycles (17β -HSD type 4).

HPLC Analysis. The hippocampal cubic slices ($1 \times 1 \times 1$ mm slices) from two rats were incubated with 5×10^6 cpm of [^{3}H] steroids at 28° C for the required hours in 2 ml of PSS containing 5 mM Hepes (pH 7.2), 0.6 mM $MgSO_4$, 0.6 mM $MgCl_2$, 137 mM NaCl, 2.5 mM $CaCl_2$, 1 mM $NaHCO_3$, 0.34 mM Na_2HPO_4, 0.44 mM KH_2PO_4, 5.36 mM KCl, and 22 mM glucose. All of the [^{3}H]steroids were purchased from New England Nuclear, and their specific activities were 17.5 Ci/mmol ([7-^{3}H] pregnenolone, PREG), 60 Ci/mmol ([1,2,6,7-^{3}H] dehydroepiandrosterone, DHEA), 95 Ci/mmol ([1,2,6,7-^{3}H]testosterone), 51 Ci/mmol ([1,2-^{3}H]dihydrotestosterone, DHT), 105 Ci/mmol ([1,2,6,7-^{3}H]androstenedione, AD), 74 Ci/mmol ([2,4,6,7-^{3}H] estrone), and 95 Ci/mmol ([2,4,6,7-^{3}H]estradiol) (1 Ci = 37 GBq). The incubation medium was gassed with 95% O_2 and 5%

CO_2 in order to keep hippocampal slices active. After termination of the reaction by chloroform, the slices were homogenized. To extract steroid metabolites, ethyl acetate/hexane = 3:2 was applied to the homogenates which were then mixed and centrifuged at $3,000 \times g$. The organic phase was collected and the extraction step was repeated twice. The combined organic extracts were dried, dissolved in methanol/water (40:60 vol/vol), and subjected to the C_{18} Amprep solid phase column (Amersham Biosciences). Unconjugated steroid fractions were dissolved in an elution solvent of HPLC, and filtrated through a membrane filter (0.45 μm: Ultrafree-MC, Millipore). The steroid metabolites (adjusted to a total of 10^6 cpm) were separated using an HPLC system (Jasco) consisting of PU2080 Pump, AS-2055 Autosampler and MD-1510 Multichannel Detector. For normal phase HPLC, a silica gel column (0.46 × 15 cm, Cosmosil 5SL, Nacalai Tesque) was used. For reverse-phase HPLC, an octadesyl-coated silica gel column (0.46 × 15 cm, Cosmosil $5C_{18}$-MS, Nacalai Tesque) was used. For monitoring of metabolite positions, 300 cpm of [^{14}C]steroids such as [^{14}C]estradiol were added to the ^{3}H-metabolites. Fraction radioactivity was measured by using a liquid scintillation spectrometer.

RIA Analysis. After the blood collection, the hippocampi were excised, sliced (1 × 1 × 1 mm slices) and transferred into PSS containing 0.1 mM Mg^{2+}. The cubic slices were incubated with or without *N*-methyl-D-aspartate (NMDA) (Biomol) in 0.1 mM Mg^{2+} PSS for 30 min at 37° C into which O_2 gas was bubbled. The slices were then homogenized, and [^{14}C]estradiol or [^{14}C] DHEA (300 cpm) was added to allow monitoring of the recovery of steroids throughout the extraction. Extraction of steroids were performed as described in *HPLC Analysis*. The collected steroids in organic solvent (ethyl acetate/hexane = 3:2) was dried, dissolved in methanol/water (40:60, vol/vol), and subjected to the C_{18} Amprep solid phase column (Amersham Biosciences). Unconjugated steroid fractions were reconstituted in HPLC solvent A, filtrated with a membrane filter, and subjected to HPLC. The separated fractions, including the peak corresponding to [^{14}C]estradiol or [^{14}C]DHEA, were collected and reconstituted in an RIA buffer (composed of 0.15 M NaCl, 0.1% gelatin, 0.02% NaN_3, and 0.1 M sodium phosphate, pH 7.0). The concentration of steroids was measured by RIA, which is a competitive reaction assay between purified estradiol (or DHEA) and exogenously added [^{3}H]estradiol against estradiol IgG (or [^{3}H]DHEA against DHEA IgG). A specific anti-estradiol IgG or anti-DHEA IgG was from ICN Biochemicals. The average recovery of estradiol and DHEA was 45% and 50%, respectively. The lower limit of detectability for estradiol and DHEA was 0.002 ng per sample and 0.01 ng per sample, respectively. As determined by the ICN RIA kit manufacturer, the cross-reactivity of anti-estradiol IgG was 0.08% with estrone, and <0.01% with other steroids such as testosterone, etc. The cross-reactivity of anti-DHEA IgG was 0.32% with androstenedione, 0.02% with androsterone and pregnenolone, and <0.01% with other steroids. The most important detail in the application of RIA for the neurosteroid assay is the removal of fats and proteins from the samples to obtain highly purified steroids prior to a competitive reaction assay between purified estradiol and exogenously added [^{3}H]estradiol against estradiol IgG, as the presence of contaminating materials interferes with the antigen-antibody reaction. In our procedures, prepurification of estradiol and DHEA from the hippocampus greatly facilitated the subsequent application of RIA. The intra- and interassay coefficients of variation were 5-7% and 9-18%, respectively, for estradiol RIA and 9-12% and 15-22%, respectively, for DHEA RIA.

As illustrated in Fig. 6, comparison of estradiol levels showed that 100 pmol of E2 per liter in plasma is roughly equal to 1 fmol E2 per 1 mg of protein in hippocampus, via the following estimation. First, 1 μl of blood is assumed to weigh   1 mg, as 1 ml of pure water weighs 1 g. Second, we assume that a brain tissue having 1 mg wet weight has an approximate volume of 1 μl, because the majority of the tissue consists of water, whose 1-ml weight is 1 g. Third, 10 mg wet weight of the hippocampal tissue contains 0.96 ± 0.02 mg of protein (see ref. 3). Direct conversion, using these values, then indicates that, within experimental error, 0.098 fmol E2 per μl (= 98 pmol/liter) in plasma is roughly 0.098 fmol/mg wet weight or 1 fmol/mg protein (= 0.098 fmol per 0.096 mg protein). Note that the true volume of brain tissue is expected to differ from this estimate by less than -10%, due to the specific volumes of proteins and lipids (0.7-0.8 ml/g). The vertical axis of Fig. 6 is drawn based on this estimation.

Results for HPLC Analysis of Additional Metabolites. To further investigate the additional pathway of steroid metabolism, [1,2,6,7-^{3}H]AD and [2,4,6,7-^{3}H]estrone were used as substrates. A significant formation of [^{3}H]testosterone from [^{3}H]AD was observed. The relative amount of [^{3}H]testosterone (product) to [^{3}H]AD (substrate) increased from $0.0 \times 10^4 : 1.0 \times 10^6$ (0 h) to $3.6 \times 10^4 : 0.87 \times 10^6$ (1 h), $8.9 \times 10^4 : 0.79 \times 10^6$ (3 h) and $9.9 \times 10^4 : 0.76 \times 10^6$ (5 h). The formation of [^{3}H]estradiol from [^{3}H]estrone was observed. The relative amount of [^{3}H]estradiol (product) to [^{3}H]estrone (substrate) increased from $0.0 \times 10^4 : 1.0 \times 10^6$ (0 h) to $0.5 \times 10^4 : 0.96 \times 10^6$ (1 h), $2.3 \times 10^4 : 0.94 \times 10^6$ (3 h) and $3.4 \times 10^4 : 0.93 \times 10^6$ (5 h).

1. Shinzawa, K., Ishibashi, S., Murakoshi, M., Watanabe, K., Kominami, S., Kawahara, A. & Takemori, S. (1988) *J. Endocrinol.* **119**, 191-200.

2. Jakab, R. L., Horvath, T. L., Leranth, C., Harada, N. & Naftolin, F. (1993) *J. Steroid Biochem. Mol. Biol.* **44**, 481-498.

3. Kimoto, T., Tsurugizawa, T., Ohta, Y., Makino, J., Tamura, H., Hojo, Y., Takata, N. & Kawato, S. (2001) *Endocrinology* **142**, 3578-3589.

Fig. 8